Real-Time Monitoring of the Transesterification of Soybean Oil and Methanol by Fourier-Transform Infrared Spectroscopy

ARTICLE *in* ENERGY & FUELS · SEPTEMBER 2013

Impact Factor: 2.79 · DOI: 10.1021/ef4012998

5 AUTHORS, INCLUDING:

Feng Zhang
Kobe University
11 PUBLICATIONS **22** CITATIONS
SEE PROFILE

Sriappareddy Tamalampudi
University of Agricultural Sciences, Bangalore
19 PUBLICATIONS **879** CITATIONS
SEE PROFILE

energy&fuels

Article

pubs.acs.org/EF

Real-Time Monitoring of the Transesterification of Soybean Oil and Methanol by Fourier-Transform Infrared Spectroscopy

Feng Zhang,[†] Daisuke Adachi,[‡] Sriappareddy Tamalampudi,[‡,∥] Akihiko Kondo,[‡] and Keisuke Tominaga*[,†,§]

[†]Graduate School of Science, [‡]Graduate School of Engineering, [§]Molecular Photoscience Research Center, Kobe University, Nada, Kobe 657-8501, Japan

ABSTRACT: Fourier-transform infrared spectroscopy with the attenuated total reflection method provides a fast, reliable technique to monitor the conversion of oil to fatty acid methyl esters (FAME) during biodiesel production. In this work, we employed a linear calibration method to monitor the generation of FAME in the transesterification of soybean oil and methanol, catalyzed by immobilized *Candida antarctica* lipase B (CALB). The interaction of the immobilized CALB catalyst with the substrates and products improved its catalytic performance. The rate law changed from zero-order in the first run to quasi-first-order in the subsequent three reaction runs. The quasi-first-order rate law was characterized by a phenomenological compressed exponential function.

1. INTRODUCTION

The biodiesel industry has developed rapidly in recent years. Fatty acid methyl esters (FAME), which are the main constituents of biodiesel, are usually produced by the transesterification of plant oil or animal fat with alcohols. The reaction is catalyzed by homogeneous alkaline or acid catalysts[1,2] or by heterogeneous catalysts such as enzymes.[3−8]

It is particularly important to determine the FAME content in reaction mixtures for industrial purposes, such as quality control and monitoring the conversion of oil to FAME, and also for academic purposes, such as reaction kinetics studies. However, these transesterification systems contain triglyceride (TG) and alcohol reactants, diglyceride (DG) and monoglyceride (MG) intermediates, and FAME and glycerin products, which makes this task challenging. Various analytical methods, including gas chromatography (GC),[9,10] gel permeation chromatography,[11] high-pressure liquid chromatography,[12] and nuclear magnetic resonance,[13] have been used in this regard. However, the measurements are time-consuming and involve complex sample preparation, limiting their utility for real-time analyses.

Infrared (IR) spectroscopy (mid-IR and near-IR) is advantageous because of its rapid data acquisition and easy sample preparation, and it is generally employed to cover the shortcomings of the above analytical methods.[14−22] In principle, the concentrations of reaction components can be determined using Beer's law, provided that their characteristic IR bands are well separated. In transesterification systems, however, reactants, products, and intermediates possess similar functional groups, which results in extensive overlap of their characteristic IR bands. In industrial methods, multivariate calibration models are often used to reduce the calibration error.[23,24] This method has been thoroughly validated in previous studies.[14−19] Nevertheless, the multivariate calibration model for a particular biodiesel reaction system requires extensive retesting when it is used for different reactant oils or catalysts, because the IR absorption patterns may vary greatly.

To simplify data processing, much effort has been devoted to searching for potential noninterfering IR bands that correspond solely to FAME. Natalello and co-workers recently found a marker band around 1435 cm^{-1} that was attributed to the CH_3 asymmetric deformation and indicated the formation of FAME.[20,21] The peak height of the second derivative of the band gave a highly linear calibration curve for FAME concentration. Similarly, de Souza and Cajaiba da Silva reported a phenomenological linear relationship between the variation of the peak height of the C−O stretching band around 1025 cm^{-1} of the methanol substrate and FAME concentration.[22] However, the independence of this band should be further examined since its asymmetric line shape suggests interference from neighboring bands. Hence, the exclusive attribution of the variation of peak height to methanol consumption, and consequently FAME generation, requires further justification. In fact, as stated by Natalello et al.,[20] the second derivative is an essential approach for examining band independence. Only a band featuring a sharp and symmetric second derivative line shape can exclusively indicate a single reaction component.[20]

In this work, we employed attenuated total reflection (ATR) Fourier-transform (FT) IR spectroscopy to monitor the transesterification of soybean oil and methanol catalyzed by immobilized *Candida antarctica* lipase B (CALB). The purpose of the study was twofold: first, to use difference spectroscopy to highlight the dynamic elements in the IR spectra in order to assist with band identification and band assignment in the fingerprint region (1000−1800 cm^{-1}); and second, to examine whether some IR bands reported in the literature[20−22] give a valid linear relationship with FAME concentration in a transesterification system catalyzed by an immobilized enzyme.

Using the established linear calibration model, we conducted a preliminary investigation of the rate law. The trans-

Received: July 9, 2013
Revised: September 5, 2013

dx.doi.org/10.1021/ef4012998 | *Energy Fuels* XXXX, XXX, XXX−XXX

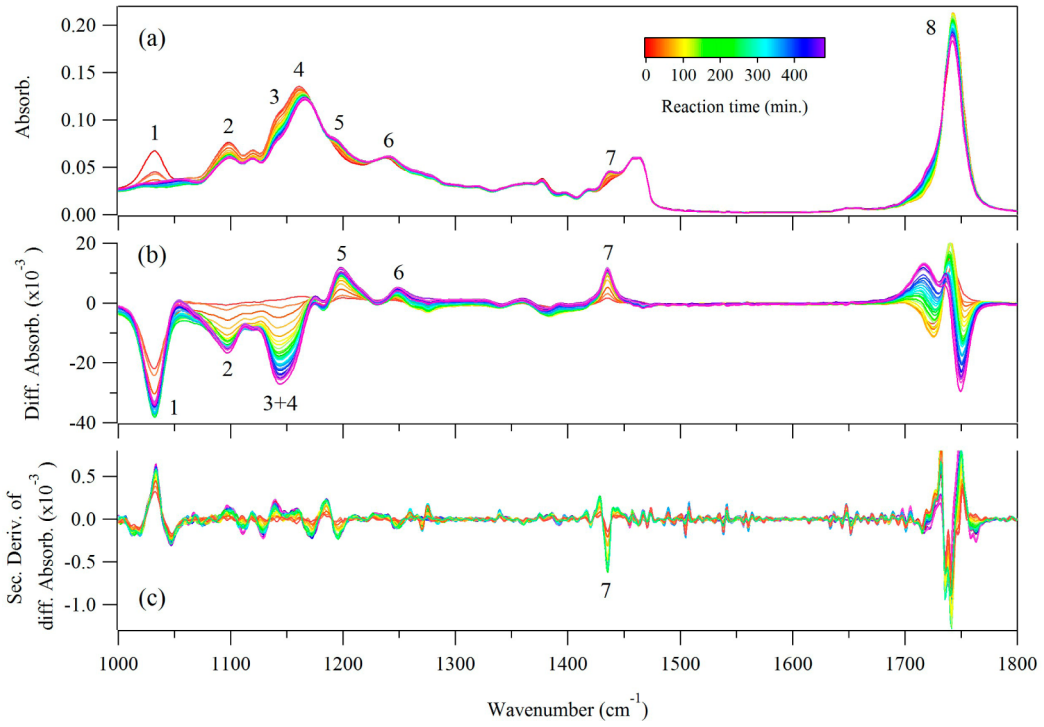

Figure 1. (a) Superposition of ATR-FTIR spectra recorded during reaction 4. (b) Superposition of difference spectra obtained by subtracting the spectrum at 0 min. (c) Superposition of the second-order derivatives of the difference spectra in part b.

esterification followed a zeroth-order rate law when catalyzed by fresh immobilized CALB but changed to a quasi-first-order rate law when catalyzed by recycled immobilized CALB. The catalytic activity of the enzyme, evaluated by a quasi-first-order rate constant, steadily improved with the number of recycling times.

2. MATERIALS AND METHODS

2.1. Materials. Methanol and immobilized CALB were purchase from Sigma-Aldrich Chemical Co. (St. Louis, MO), and refined soybean oil was purchased from Wako Pure Chemical Co. (Osaka, Japan).

2.2. Transesterification. The experimental procedure followed the first step in the three-step reaction reported by Shimada et al.[4] Prior to the reaction, a mixture of 0.2 mol of soybean oil and 0.2 mol of methanol in a 50 mL screw-capped vessel was heated to 30 °C and homogenized at 130 oscillation/min. Immobilized CALB (5 wt % with respect to soybean oil) was warmed to 30 °C and then added to the vessel to initiate the reaction. The experiment ran for 480 min. During the course of the reaction, 0.1 mL samples were collected from the supernatant at 0 min and then every 10 min during the first 2 h, every 20 min during the next 2 h, and then every 30 min during the last 4 h. Finally, the reaction mixture was centrifuged at 5000 rpm for 5 min to separate the immobilized CALB, which was washed with fresh soybean oil three times and stored in biodiesel. The biodiesel, which was the final product of the above three-step reaction and had a FAME content of more than 98%, was prepared by the Osaka Municipal Technical Research Institute. The reaction was then repeated once a week using the CALB recycled from previous runs, for three runs. The immobilized CALB was stored in biodiesel at 4 °C. Before use, it was washed by fresh soybean oil three times and then incubated at 30 °C for half an hour. The four runs were numbered 1−4 in order of time. The whole process was repeated once to check its reproducibility.

2.3. Analysis. ATR-FTIR spectra of all the samples without further treatments were recorded using an FTIR-6100 spectrometer (JASCO) equipped with a ZnSe crystal ATR PRO410-S sampling accessory (JASCO). For each sample, 256 scans were taken from 400 to 4000 cm^{-1} at a resolution of 4 cm^{-1}. Traces of atmospheric CO_2 and water vapor were removed using the built-in processing software. After measurement, the surface of the ZnSe crystal was cleaned successively with dichloromethane, methanol, and water.

GC analyses were performed on a GC-2014 gas chromatography system (Shimadzu, Kyoto, Japan). The methyl ester content was analyzed using a DB-5 capillary column (0.25 mm × 15 m; Phenomenex, Torrance, CA). The temperatures of injector and detector were 245 and 320 °C, respectively. The column temperature program was as follows: 150 °C for 0.5 min; increase to 300 °C at a rate of 10 °C/min; and 300 °C for 5 min.

3. RESULTS AND DISCUSSION

3.1. IR Spectra. Figure 1a shows the IR spectra recorded during reaction 4 in the range 1000−1800 cm^{-1}. The IR spectra of the three other reactions are not presented here. As expected for this complex reaction system, the IR bands in the fingerprint region were broad and overlapped. During the reaction, some of the bands showed time-dependent intensities or wavenumbers, or both. We focused on the eight bands which showed significant time dependence; they were numbered 1−8 in order of wavenumber.

To highlight the variation elements of the spectra, the 0 min spectrum was subtracted from each spectrum taken during the reaction, and the resulting difference spectra are shown in Figure 1b. The dynamic processes in the reaction were indicated by the negative and positive signals in the difference spectra. During the reaction, the number of terminal methyl groups does not change. This was true for most of the other bands, specifically, (O═)C−O−C and C−C(═O)−O. Therefore, if the absorption coefficients, frequencies, and line shapes were the same for vibrational modes before and after the reaction, no signals should be visible in the difference spectra. However, positive or negative bands were visible, indicating

dx.doi.org/10.1021/ef4012998 | Energy Fuels XXXX, XXX, XXX−XXX

Table 1. Assignments of the Seven Vibrational Bands Showing Strong Time Dependence and Assignments Reported in Refs 17 and 19[a]

band	assignment		frequency (cm^{-1}) this work	ref 17	ref 19
1	C−O str in C−OH	methanol	1010−1050		
2	O−C str in O−CH_2C	MG, DG, TG	1075−1110	1100	1075−1111
3	O−C str in O−CHC_2	MG, DG, TG	1130−1147		
4	asym C−O−C str in ester bonds	MG, DG, TG, FAME	1150−1175	1170	
5	O−C str in O−CH_3	FAME	1183−1220	1200	1188−1200
6	asym C−C(=O)−O str in ester bonds	MG, DG, TG, FAME	1220−1260		
7	CH_3 asym def in O−CH_3	FAME	1424−1448	1445	1425−1447
8	C=O str	MG, DG, TG, FAME	1690−1780		1700−1800

[a]Soybean oil was used in this work and in ref 17; a mixture of cotton, sunflower, and sesame seed oil was used as the reactant in ref 19.

differences in the absorption coefficient, frequency, and line shape of vibrational groups between the products and reactants.

Although rigorous band assignment can be carried out by examining frequency shifts arising from isotopic substitution and by conducting normal-mode analysis, it is beyond the scope of this study. Bands were tentatively assigned to account for the dynamic information revealed in the difference spectra. Band 1 was assigned to the C−O stretch of methanol. Band 2 was assigned to the O−C stretch of O−CH_2C, and the higher frequency band 3 was assigned to the O−C stretch of O−CHC_2, because branched carbons in ester bonds increase the frequency.[25,26] Band 4 was attributed to the mode involving the interaction of the (C=O)C−O−C antisymmetric stretch with the C−C motion, although for simplicity we refer to this mode as the (C=O)C−O−C antisymmetric stretch.[25,26] Bands 5 and 7 were assigned to the O−C stretch and the CH_3 asymmetric deformation of the FAME O−CH_3 group, respectively, as suggested by Siatis et al. and Mahamuni and Adewuyi[17,19] Band 6 may correspond to the C−C(=O)−O antisymmetric ester bond stretch.[25] Band 8 was confidently assigned to the C=O stretch. The assignments of bands 1−8 are summarized in Table 1 together with the band locations in refs 17. and 19.

The intensities of band 1 and bands 2 and 3 decreased continuously, indicating the consumption of the methanol and TG reactants, respectively. Band 4 gradually shifted to a higher frequency, and was specifically related to the transesterification, during which the α-carbon-fragments, $-CH_2C$ and $-CHC_2$, of the ester bonds were substituted with a methyl group, $-CH_3$. The transesterification blue-shifted this mode, because of the reduction in mass. The gradual increase in the intensity of bands 5, 6, and 7 relates to the formation of FAME.

Bands 1, 2, 5, and 6 had asymmetric line shapes in the difference spectra; bands 3 and 4 combined to form a broad asymmetric band. The asymmetric line shapes arose mainly from interference with neighboring bands, as well as from subtle changes in the vibrational frequencies, molar absorption coefficients, and line shapes of the corresponding functional groups caused by interactions with the dynamic environments. Band 8, representing the C=O stretch shared by all substrates and products, showed a complicated multicomponent variation pattern in the difference spectra, implying the vigorous dynamic process that this functional group experienced during the reaction. Band 7 was the only band featuring a perfectly symmetrical line shape in the difference spectra, providing preliminary evidence that it was free of interference with other bands.

This assertion was proved by taking the second derivative of the difference spectra, as shown in Figure 1c, which is a general approach for decomposing components of a coupled band. In contrast to the other seven bands, the second derivative of band 7 appeared distinctively sharp and symmetric, firmly demonstrating its correspondence to only CH_3 asymmetric deformation. Furthermore, this observation disproved that any other bands had a linear relationship with the time course of transesterification. This result is consistent with the conclusion reached by Natalello et al.[20] and Santambrogio et al.,[21] and the explanation is straightforward: having a symmetric electron configuration and weak dipole moment, the CH_3 group was unlikely to interact strongly with other functional groups, and consequently, it maintained a constant center frequency and molar absorption coefficient. Hence, free from the interference with other bands, band 7 corresponded exclusively to the vibration of the CH_3 group in FAME. The concentration of FAME was consequently related to the band height of band 7 through Beer's law, assuming the penetration depth of the IR beam around 1436 cm^{-1} was constant for all samples.

The time dependence of band height in the difference spectra is shown in Figure 2. There were three negative curves corresponding to bands 1 and 2 and the combined bands 3 and 4 (Figure 2a). In addition, there were three other positive curves corresponding to bands 5−7 (Figure 2b). The time dependence of band 8 is not shown due to its overly complex variation pattern. The time evolution of the weight percentage of FAME measured by GC is plotted in Figure 3a. Of the six bands, the time dependence of band 7 was most similar to that of the FAME weight percentage, indicating the reliability of band 7's correspondence to FAME production.

Furthermore, the relationship was confirmed by the quantitative fitting of the two curves by a phenomenological compressed exponential function

$$f(t) = C_0(1 - \exp(-(kt)^{\beta})) \quad (1)$$

where $f(t)$ is the band height of band 7 in Figure 2b and the weight percentage of FAME in Figure 3a, C_0 is the plateau values of the two curves, k is a quasi-first-order rate constant, and β is a compressing exponent. The combination of the fitting parameters (k,β) contains the overall kinetic information for this reaction.

The fitting results are shown in Table 2. The values of k and β for the two curves agreed well. The differences were measured as 0.8% for k, and 3% for β, respectively, with reference to the GC measurements. The consistent fitting

dx.doi.org/10.1021/ef4012998 | Energy Fuels XXXX, XXX, XXX−XXX

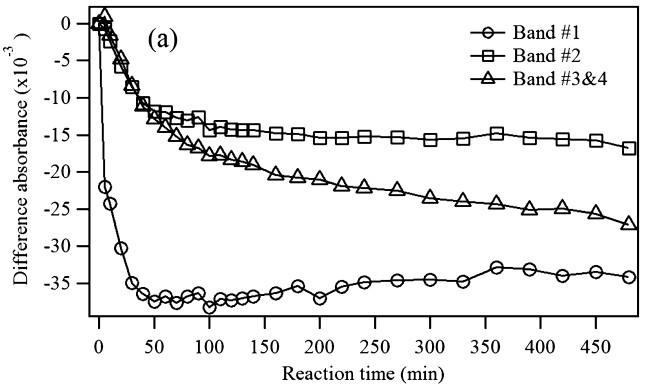

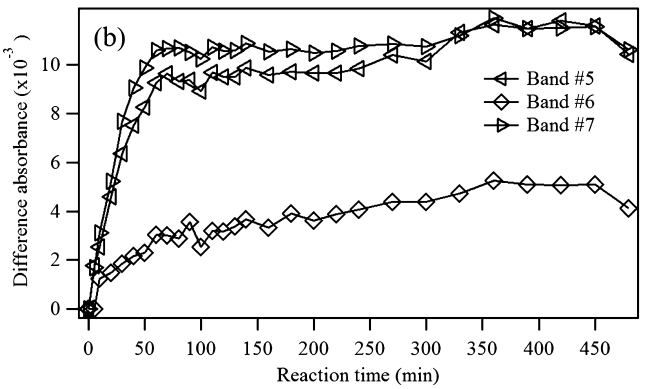

Figure 2. Variation of the band heights of the difference bands during reaction 4. (a) The three negative difference bands corresponding to bands 1 and 2 and the combination of bands 3 and 4. (b) The three positive difference bands corresponding to bands 5−7.

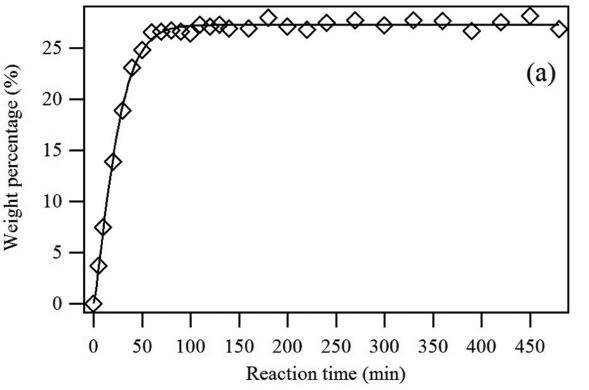

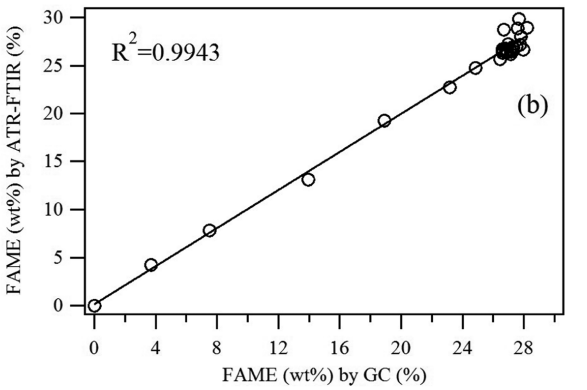

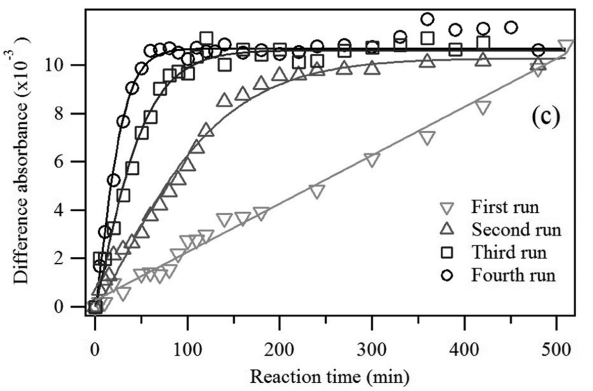

Figure 3. (a) Variation of the weight percentage of FAME during reaction 4 measured by GC and the fitting curve using eq 1. The fitting covers the entire range. (b) Correlation between the weight percentages of FAME determined by ATR-FTIR and measured by GC. (c) Variation of the band height of band 7 in the difference spectra during reactions 1−4. Reaction 1 is fitted with a linear function passing through the origin. Reactions 2−4 are fitted with eq 1. The fitting covers the entire range.

results demonstrate that the IR curve actually described the changes in FAME concentration. Therefore, the band height of band 7 in the difference spectra provides a reliable method for measuring the concentration of FAME. Figure 3b shows the linear calibration relationship between the weight percentage of FAME predicted by FTIR and that measured by GC.

The conclusion arrived at in this work is in full agreement with that of Natalello et al.[20] and Santambrogio et al.[21] Since they used an aqueous enzyme solution for catalysis, the hydrolysis of TG was a possible side reaction in that case. In fact, band 7 barely interfered with the reactants and products, with the oleic acid side products, and with water. This finding provides an insight into applying this method to potential oil sources that might contain high concentrations of water and free fatty acids, such as recycled industrial or restaurant grease. In another case of transesterification using potassium hydroxide as the catalyst, the marker band around 1436 cm^{-1} was also observed to grow while maintaining a symmetric line shape during the reaction.[19] On the basis of the overall observations, we reached the conclusion that the independent CH_3 asymmetric deformation band of FAME is a general feature of the IR spectra for transesterification, regardless of the oil and alcohol substrates and catalyst. This linear calibration method should be valid for general application in the biodiesel field.

3.2. Rate Law. The time evolution of the band heights of band 7 in difference spectra in reactions 1−4 is shown in Figure 3c. Reaction 1 followed a zero-order law, indicated by the linear relationship and a constant reaction rate of 2.00×10^{-5} ($\pm 4.31 \times 10^{-7}$) min^{-1}, implying the CALB catalyst limited the rate at this stage. The initial rate of reaction increased from reaction 2 onward, and the rate law changed accordingly. This indicates that the CALB catalyst activity increased, and it was no longer a rate-limiting factor.

Table 2. Fitting Results Using Eq 1

measurement	reaction	k ($\times 10^{-2}$ min^{-1})	β
ATR-FTIR	2	0.95 ± 0.043	1.26 ± 0.0753
	3	2.23 ± 0.097	1.18 ± 0.0809
	4	3.92 ± 0.175	1.22 ± 0.0875
GC	4	3.95 ± 0.0783	1.26 ± 0.0416

dx.doi.org/10.1021/ef4012998 | Energy Fuels XXXX, XXX, XXX−XXX

Equation 1 was also found to be suitable for fitting the time dependence curves in reactions 2 and 3. The fitting results are shown in Table 2 along with those for reaction 4. For all the three reactions, the compressing exponential β was around 1.2. This implies they may obey the same rate law. The quasi-first-order rate constant k gradually increased with the reaction time, implying the performance of the CALB improved. This finding sheds light for improving the efficiency of industrial practices and for revealing the reaction mechanisms.

Finally, we will use the phenomenological observations for a preliminary discussion of the rate law. After reaction 2, the catalytic performance of the immobilized CALB improved because of the interactions with the substrates and products during the reaction and storage. The longer the interactions lasted, the better the performance. Similar phenomena have been reported when the immobilized CALB was immersed in oil, FAME, or butanol to improve the catalytic velocity.[4,5] Although the interaction mechanism is still unclear, the following are possible explanations: (1) the region of the CALB inactivated by attachment to the matrix is activated by interactions between the enzyme, matrix, substrates, and products; (2) the enzyme inhibition is reduced; and (3) the external and internal diffusion limitations are reduced. Enzyme inhibition and limited diffusion counteract each other if they occur simultaneously. On balance, these two processes result in a net increase in the catalytic activity of CALB. This demonstrates that the interface interactions in a heterogeneous system, and the interactions between the enzyme and the embedding matrixes, strongly influence the rate of reaction and should not be neglected in kinetic studies of embedded CALB. Direct use of well-accepted models for homogeneous phase catalysis, such as the Michaelis–Menten model or the Ping-Pong Bi Bi model, will oversimplify the reaction.[27]

4. CONCLUSION

The transesterification of soybean oil and methanol catalyzed by immobilized CALB was monitored by ATR-FTIR spectroscopy in real time. Bands were assigned to account for the dynamic information revealed by the difference spectra in the fingerprint region. We proved the validity of the linear calibration model proposed by Natalello and co-workers[20,21] by performing transesterification catalyzed by the immobilized enzyme. The results suggest broader application is feasible in biodiesel production, regardless of the oil and alcohol substrates and catalyst.

The catalytic performance of immobilized CALB was enhanced through its interactions with substrates and products. The rate law was zero-order during the first run of the reaction, and quasi-first-order during the three subsequent runs, which were well fitted with a compressed exponential function. The quasi-first-order rate constant k reflects the performance of the immobilized CALB. The fluctuation of compressing exponent β around 1.2 may indicate that the last three reactions followed the same rate law.

AUTHOR INFORMATION

Corresponding Author

*Address: Molecular Photoscience Research Center, Kobe University, Nada, Kobe 657-8501, Japan. E-mail: tominaga@kobe-u.ac.jp. Tel.: +81-78-803-5684. Fax: +81-78-803-5684.

Present Address

[||]Biofuel Research Laboratory, Department of Plant Biotechnology, University of Agricultural Sciences, GKVK, Bangalore 560065, India.

Notes

The authors declare no competing financial interest.

REFERENCES

(1) Ejikeme, P. M.; Anyaogu, I. D.; Ejikeme, C. L.; Nwafor, N. P.; Egbuonu, C. A.; Ukogu, K.; Ibemesi, J. A. *Eur. J. Chem.* **2010**, *7* (4), 1120–1132.

(2) Zhang, Y.; Dubé, M. A.; Mclean, D. D.; Kates, M. *Biosesour. Technol.* **2003**, *89* (1), 1–16.

(3) Shimada, Y.; Watanabe, Y.; Samukawa, T.; Sugihara, A.; Noda, H.; Fukuda, H.; Tominaga, Y. *J. Am. Oil Chem. Soc.* **1999**, *76* (7), 789–793.

(4) Shimada, Y.; Watanabe, Y.; Sugihara, A.; Tominaga, Y. *J. Mol. Catal. B: Enzym.* **2002**, *17*, 133–142.

(5) Du, W.; Xu, Y. Y.; Zeng, J.; Liu, D. H. *Biotechnol. Appl. Biochem.* **2004**, *40*, 187–190.

(6) Du, W.; Xu, Y. Y.; Liu, D. H.; Zeng, J. *J. Mol. Catal. B: Enzym.* **2004**, *30*, 125–129.

(7) Chang, H. M.; Liao, H. F.; Lee, C. C.; Shieh, C. J. *J. Chem. Technol. Biotechnol.* **2005**, *80*, 307–312.

(8) Fjerbaek, L.; Christensen, K. V.; Norddahl, B. *Biotechnol. Bioeng.* **2009**, *102* (5), 1298–1315.

(9) Knothe, G. *Am. Soc. Agric. Eng.* **2001**, *44* (2), 193–200.

(10) Plank, C.; Lorbeer, E. *J. Chromatogr., A* **1995**, *697*, 461–468.

(11) Mittelbach, M. *Chromatographia* **1993**, *37* (11), 623–626.

(12) Holčapek, M.; Jandera, P.; Fischer, J.; Bořivoj, P. *J. Chromatogr., A* **1999**, *858*, 13–31.

(13) Knothe, G. *J. Am. Oil Chem. Soc.* **2000**, *77* (5), 489–493.

(14) Zagonel, G. F.; Peralta-Zamora, P.; Ramos, L. P. *Talanta* **2004**, *63*, 1021–1025.

(15) Knothe, G. *J. Am. Oil Chem. Soc.* **1999**, *76* (7), 795–800.

(16) Richard, R.; Li, Y.; Dubreuil, B.; Thiebaud-Roux, S.; Prat, L. *Bioresour. Technol.* **2011**, *102*, 6702–6709.

(17) Siatis, N. G.; Kimbaris, A. C.; Pappas, C. S.; Tarantilis, P. A.; Polissiou, M. G. *J. Am. Oil Chem. Soc.* **2006**, *83* (1), 53–57.

(18) Trevisan, M. G.; Garcia, C. M.; Schuchardt, U.; Poppi, R. J. *Talanta* **2008**, *74*, 971–976.

(19) Mahamuni, N. N.; Adewuyi, Y. G. *Energy Fuels* **2009**, *23*, 3773–3782.

(20) Natalello, A.; Sasso, F.; Secundo, F. *Biotechnol. J.* **2013**, *8*, 133–138.

(21) Santambrogio, C.; Sasso, F.; Natalello, A.; Brocca, S.; Grandori, R.; Doglia, S. M.; Lotti. M. *Appl. Microbiol. Biotechnol.* 2013; http://dx.doi.org/ 10.1007/s00253-013-4712-5.

(22) De Souza, A. V. A.; Cajaiba Da Silva, J. F. *Org. Process Res. Dev.* **2013**, *17* (1), 127–132.

(23) Miller, C. E. *Chemom. Intell. Lab. Syst.* **1995**, *30*, 11–23.

(24) Martens, H.; Naes, T. *Multivariate Calibration*; John Wiley: Chichester, 1993.

(25) Günzler, H.; Gremlich, H. U. *IR Spectroscopy—An Introduction*; Wiley-VCH: Germany, 2002.

(26) Socrates, G. *Infrared characteristic group frequencies*; Wiley: England, 1994.

(27) Samukawa, T.; Kaieda, M.; Matsumoto, T.; Ban, K.; Kondo, A.; Shimada, Y.; Noda, H.; Fukuda, H. *J. Biosci. Bioeng.* **2000**, *90* (2), 180–183.